Focus Review for Polymer Journal

Angle-independent Colored Materials Based on the Christiansen Effect Using Phase-Separated Polymer Membranes

Yukikazu Takeoka

Department of Molecular Design & Engineering, Nagoya University, Furo-cho, Chikusa-ku, Nagoya, 464-8603, Japan
E-mail: ytakeoka@apchem.nagoya-u.ac.jp

Herein, I review the fabrication of new optical composites that exhibit color changes without dyes or pigments covering the whole visible region in response to temperature via changes in both the diffraction properties and the wavelength dispersion of their refractive indices. These systems, which are composed of porous polymer membranes and thermosensitive liquids, display bright coloration caused by the Christiansen effect because the wavelength dispersion of the polymer membranes and the liquids intersect in the visible region. The thermally tunable coloration of the porous polymer membranes containing thermosensitive liquid arises from the coincidence at one wavelength of the dispersion curves of the porous polymer membranes and the thermosensitive liquid portions and depends on the composition and temperature of the thermosensitive liquid.

INTRODUCTION

Inspired by the existence of living things that display angle-independent structural colors, our group has attempted to produce such a property in artificial materials to produce biomimetic or bio-inspired structurally colored materials[1-12]. In particular, we have focused on angle-independent structurally colored biological tissues that are composed of monodisperse submicron spherical particles or air cavities with only short-range order. Among the structurally colored biological tissues, the angle-independent structural colors in feathers of the bluebird have been the most frequently investigated by many research groups over a long period[13-16]. According to a recent report on blue bird feathers, these feathers are self-assembled by arrested phase separation[14]. That is, the materials are not preliminarily produced, as in the case of colloidal particle assembly experiments that we often use to prepare colloidal amorphous arrays that display angle-independent structural colors. This self-assembly process within blue bird feathers produces material with isotropic short-range order without producing actual finite objects, such as sphere assemblies or channel structures. Fundamentally, this self-assembly is a one-step method that entirely differs from the two material processing steps that we use to prepare colloidal particle aggregations—specifically, making and assembling colloidal particles. In fact, the air cavity structure of blue bird feathers is not only made in a single process, but it is more optically efficient than an artificial sphere assembly. Therefore, birds still substantially outperform our current capability for materials synthesis.

Attempts to elucidate the mechanisms associated with biological materials often lead to the development of new materials that exhibit unique and notable functions. Indeed, we have developed new angle-independent colored materials not only without using pigments or dyes but also without nanostructures on the order of the magnitude of optical wavelength[17,18]. This research on the development of artificial angle-independent colored materials with phase-separated structures has resulted in the development of a new type of angle-independent colored material using the Christiansen effect[19,20]. The Christiansen effect, which was discovered by Christian Christiansen in 1884, is the reduced scattering of multi-phase microstructures at wavelengths where their refractive indices match. In many previous reports, the Christiansen effect in the infrared region has taken center stage. However, with the selection of the combination of materials, we can observe bright angle-independent

color from a system caused by the Christiansen effect. Because chromogenic development using the Christiansen effect does not require precise structural control for the preparation of colored materials, we can easily obtain angle-independent colored materials simply by choosing a combination of materials that results in the appropriate dispersion of wavelength-dependent refractive indices. No biological organisms with coloration caused by the Christiansen effect have yet been discovered. Thus, such colored materials are man-made materials developed on the basis of a principle not observed in biological systems. In this review, I explain our studies of stimuli-responsive angle-independent colored systems based on the Christiansen effect using phase-separated porous polymer membranes; these systems may be applicable to sensing and display devices.

PREPARATION OF PHASE-SEPARATED POROUS POLYMER MEMBRANES

First, I explain how to prepare phase-separated porous polymer membranes for fabricating angle-independent colored materials that operate on the Christiansen effect using different two methods: spinodal decomposition and nuclear formation.

In a typical experiment to prepare phase-separated porous polymer membrane by spinodal decomposition, we used a polymerization-induced phase separation method. To prepare such a system, we loaded a small flask with 2-(2-methoxyethoxy)ethyl methacrylate (MEO2) as a liquid monomer and 4,4′-dinonyl-2,2′-dipyridyl as a ligand molecule for the polymerization catalyst. After this sample was sealed with a stopcock and cycled several times between inert gas and vacuum to remove dissolved oxygen (which may retard polymerization), methyl-2-bromopropionate was added as an initiator to the solution. CuBr was then added as a catalyst. The solution in the small flask was placed into an isothermal bath at 20 °C, and reversible deactivation radical polymerization proceeded for approximately 20 h. As a result, phase separation was observed to accompany the polymerization in this system. The phase-separated porous polymer membrane obtained was washed with an appropriate solvent and dried to obtain an opaque porous polymer membrane.

The microstructure of the resultant porous polymer membrane, as observed by scanning electron microscopy (SEM), is self-assembled by the phase separation of

poly(MEO2) in conjunction with the polymerization of MEO2 without a solvent below 20 °C (Figure 1a). With respect to the channel-type phase-separated microstructure formed in the porous polymer membrane, the phase separation may be caused by spinodal decomposition. The phase-separated microstructure is perhaps stabilized, probably through the unexpected cross-linking reaction of poly(MEO2) because the microstructure of the porous polymer membrane, swollen slightly in toluene, is unaltered despite the lack of a cross-linker. The microstructure is composed of the isotropic channel with a characteristic length of approximately 10 μm, which is substantially larger than the wavelength of visible light. We can parameterize the size of a scatterer by the ratio between the characteristic length r and the intended wavelength of light λ: $\alpha = 2\pi r/\lambda$. The geometrical optics approximation can be used to evaluate the interaction between the scatterer and the irradiated light when the value of α becomes substantially greater than unity. Thus, we can treat this porous polymer membrane as a diffuse reflective material.

In a typical experiment to prepare phase-separated porous polymer membrane by nuclear formation, we loaded a small flask with *N*-methyl methacrylamide (MMAA) as a monomer, *N*,*N*′-methylene-bis-acrylamide (BIS) as a cross-linker, methanol as a good solvent and a certain amount of hexane as a poor solvent for polyMMAA. After inactive gas was bubbled through the solution to remove dissolved oxygen, azobisisobutyronitrile was added to the solution as an initiator for the polymerization reaction. The solution was then placed in an isothermal bath at 60 °C for approximately 20 h to prepare a different type of porous polymer membrane. Another porous polymer membrane composed of MMAA and BIS was obtained using hexane as a porogenic solvent. An SEM image of the porous polymer membrane is shown in Figure 1b. The microparticles in the porous polymer membrane become enlarged with increasing amount of the additive hexane. A dried porous polymer membrane composed of microparticles larger than 500 nm becomes opaque. With respect to the morphologies of the phase-separated structure of the porous polymer membrane, the microstructures must be induced by nuclear formation, whereas growth occurs through polymerization. We used the aforementioned two types of porous polymer membranes with appropriate conditions as diffuse reflective materials.

OPTICAL PROPERTIES OF POROUS POLYMER MEMBRANES BASED ON THE CHRISTIANSEN EFFECT

First, I will explain the optical properties of the porous polymer membrane of MEO2 in solvents. The transmittance spectra of the porous polymer membrane in different toluene-acetone mixed solvents at approximately 20 °C are shown in Figure 2a. In pure toluene (indicated as "100%"), the hue of the porous polymer membrane becomes bright blue (Figure 2b). The shape of the transmission spectra of the porous polymer membrane in 100% toluene indicates that the blue color is attributable to the diffuse reflection of shorter wavelengths of visible light. The position of the peak observed in the transmission spectra shifts to a shorter wavelength and the shape of the peak sharpens with increasing acetone content in the mixed solvent (Figure 2a). The hue of the porous polymer membrane varies depending on the composition of the mixed solvent (Figure 2b). Notably, light of a certain wavelength range where the peak is observed in the spectra could pass through the sample as a function of the solvent composition. Thus, the color from the sample must be caused by the diffuse reflection of visible light with wavelengths that are both shorter and longer than the peak position. As previously mentioned, the porous polymer membrane is slightly swollen with the solvents, whereas the pores are filled with the solvents. Therefore, the diffuse reflection of visible light must be caused by the phase-separated structure. This color phenomenon is entirely different from that of the fine structures in feather barbs or the colloidal amorphous array composed of submicron spherical particles with short-range order. In the cases of the transmission spectra of the feather barbs and colloidal amorphous arrays, a downward peak, which is caused by coherent scattering from the microstructures, is observed. The transmission spectra monitored as the irradiation angles were varied for the porous polymer membrane in 85 wt% toluene mixed solvent are shown in Figure 2c. The peak observed at 430 nm does not depend on the irradiation angle. Indeed, this porous polymer membrane in this mixed solvent displays angle-independent colors to the eye.

The temperature-dependent dispersion curves of the 10 wt% linear polymer solution, which is associated with the swollen polymer portion of the porous polymer membrane, and the dispersion curves of pure toluene at different temperatures were collected; they are compared in Figure 3a. Cauchy's approximate formula[21] was used to determine the dispersion curves for each state (solid lines), followed by identification of

the position of the intersection between the two curves with the temperature change. The estimated intersections between the dispersion curve for the 10 wt% polymer solution and that for pure toluene at each temperature were compared with the position of the peak wavelength of the transmission spectra of the porous polymer membrane in toluene at each temperature. The peak position of the transmission spectra is shifted to a shorter wavelength within the visible region, and the peak becomes sharper with increasing temperature from 25 °C to 55 °C (Figure 3a). When the refractive indices of the swollen-polymer portion and pure toluene are equal, the wavelength of light near the intersection is transmitted through the sample, whereas the other wavelengths of light are scattered. Consequently, we can observe an enhanced peak in the transmission spectra of the porous polymer membrane in pure toluene. The intersections between the two dispersion curves reflect the behavior of the peak position of the transmission spectra with change in temperature (Figure 3b). Figure 3a suggests that the sharpness of the peak may be caused by the intersection of two dispersion curves with large angles. These results indicate that the colors are caused by the Christiansen effect.

Thus far, only a few systems that enable the fabrication of visible optical filters that operate on the Christiansen effect have been reported[22] despite the Christiansen effect having been understood for well over 100 years[19]. However, the system described in the present work is easy to prepare in the form of a large display because of its straightforward preparation method and its mechanism of coloration. I believe that this colored system represents a promising new optical system for the manufacture of reflective full-color displays with a wide viewing angle, energy-saving performance, and non-fading color. In the next section, the application of the Christiansen effect caused by a porous polymer membrane with liquid crystals (LCs) for constructing a display system is presented.

APPLICATION OF POROUS POLYMER MEMBRANE TO POLYMER-DISPERSED LIQUID CRYSTAL (PDLC)

Display systems with polymer-dispersed liquid crystals (PDLC) are one of the most inexpensive and the simplest candidates for this technology[23]. Although the PDLC is relatively simplified system because of the absence of a polarizing plate or alignment film, there is still potential for improvement.

Stimuli-sensitive, multi-colored materials are potential candidates for the perfect display without a color filter[24-30]. The following section describes the preparation of a full-color PDLC system employing the aforementioned porous polymer membrane that displays bright angle-independent colors via the Christiansen effect.

In PDLC devices, the LC droplets, which are trapped in a porous portion of a polymer membrane, scatter visible light because of the mismatch of the refractive index between the LC droplets and the polymer portion. As a result, the PDLCs act as light shutters, which can alter their light transmission properties. The LC droplets can reversibly change between opaque and clear states. If we can provide other functions to the PDLC, such as the ability to exhibit different hues, PDLC devices can find application as multi-color displays. To demonstrate this concept, we used the aforementioned system that operates on the Christiansen effect.

I previously described how the porous polymer membrane immersed in an appropriate solvent displays saturated angle-independent colors by means of the dispersion curves of the swollen polymer portion and the solvent portion coinciding at one wavelength. The same type of colored system can be created by the combination of the porous polymer membrane and an appropriate isotropic LC on the basis of the same mechanism. Thus, the dispersion curve of the appropriate isotropic LC should intersect with the dispersion curve of the polymer material that forms the porous polymer membrane at a certain wavelength in the visible range. In our study, we used a porous polymer membrane composed of the MMAA-BIS polymer formed by nuclear formation. Before choosing an appropriate isotropic LC, we must determine the wavelength-dependent refractive indices of the polymer material. The dispersion curves of the MMAA-BIS polymer at two different temperatures are shown in Figure 4a. The dispersion curves of the two types of popular thermosensitive LCs (4-cyano-4′-pentylbiphenyl (5CB) and 4-(*trans*-4-pentyl-cyclohexyl)benzonitrile (5PCH)) above these isotropic points are also shown at different temperatures. The numeric data for these LCs are quoted from the literature[31]. The MMAA-BIS polymer cannot achieve a swollen state with either LC or the mixture. The dispersion curves of MMAA-BIS polymer at 25 °C and at 50 °C in the visible region are almost identical. By contrast, the changes in the dispersion curves of the liquid crystals in response to changes in the temperature are substantial compared with that of the MMAA-BIS

polymer. This result indicates that the dispersions of these LCs are thermosensitive, whereas that of the MMAA-BIS polymer is insensitive to temperature. To display the color of the porous polymer membrane composed of the MMAA-BIS polymer filled with an isotropic LC, as produced by the Christiansen effect, the dispersion curve of the isotropic LC above its isotropic point can intersect with that of the MMAA-BIS polymer in the visible range. However, pure 5CB and pure 5PCH do not satisfy the conditions necessary for fabricating the desired color display using the porous polymer membrane composed of the MMAA-BIS polymer. If we find an appropriate isotropic thermosensitive LC that satisfies the requirements, a multi-color PDLC can be attained.

Here, I explain the protocol for fabricating a multi-color PDLC using the porous polymer membrane and a thermotropic LC mixture. Figure 4b shows the conceptual scheme of a typical thermotropic LC, illustrating the temperature dependence of the refractive index at a certain wavelength. In the case of a thermotropic LC, at temperatures below the isotropic point (T_{NI}), the LC can form ordered states and exhibit double refraction. At temperatures above T_{NI}, a thermotropic LC exhibits its isotropic liquid nature and has only one refractive index at each temperature at a certain wavelength. In Figure 4c, the experimental refractive index at several wavelengths is plotted versus temperature for 5CB and 5PCH as LCs. Both compounds are thermotropic LCs that exhibit phase transitions from the isotropic phase to the nematic LC phase with decreasing temperature, as shown in Figure 4b. The values of T_{NI} between the nematic phase and the isotropic phase of 5CB and 5PCH are approximately 33 °C and 53 °C, respectively. As previously mentioned, these pure LCs are not useful for preparing the desired multi-color PDLC when using the MMAA-BIS polymer. However, the thermotropic LC phase transition can be observed not only in these pure states but also in their mixtures. The differential scanning calorimetry (DSC) results and the optical observations for each compound and the mixtures are shown in Figure 5. Two endothermic peaks are observed for each pure LC from 10 °C to 60 °C in the DSC thermograms. The lower and upper peaks correspond to the melting point (T_m) and T_{NI}, respectively. The T_m values of pure 5CB and pure 5PCH are approximately 18 °C and 29 °C, respectively. However, the melting points of the mixtures are lower than both of these values because of their eutectic properties, whereas the T_{NI} of the mixed LCs continuously varies from 33 °C to 53 °C as a function of the composition. Therefore, the LC ranges of the mixtures become wider than the ranges of the pure compounds. As

a result, this condition provides an excellent effective temperature region for the PDLC. Additionally, the position of the dispersion curve for the isotropic state of the mixture can be easily controlled via the mixing ratio of these LCs. Thus, we can obtain a desired LC mixture that satisfies the appropriate conditions to prepare a temperature-controlled multi-color PDLC.

If the LC mixtures fill the porous portion in the polymer membrane, then, at temperatures below the T_{NI} of the LC mixtures, these resultant composites will strongly scatter visible light across whole region because of the mismatches in the refractive indices between the polymer portion and the LC mixtures. Hence, this composite system becomes an opaque material. However, at temperatures above the T_{NI}, the porous polymer membrane filled with the isotropic LC mixtures can display colors under the conditions where the dispersion curve of the isotropic LC intersects with that of the MMAA-BIS polymer in the visible region. Figure 6a shows the temperature-dependent transmission spectra of the MMAA-BIS porous polymer membrane filled with the LC mixture with 73% 5PCH. This LC mixture exhibits a T_{NI} of 42 °C (see Figure 5). At temperatures below 42 °C, the composite system scatters optical wavelengths across whole region when the LC mixture is in a nematic state. As a result, the composite system becomes opaque (see the data at 40 °C in Figure 6b). In stark contrast, a certain peak caused by the Christiansen effect appeared at temperatures above the T_{NI} in each transmission spectrum (Figure 6a). Additionally, the position of the peak is moved reversibly when the temperature is changed; this movement is induced by the change in the intersection point of the two dispersion curves. Thus, the composite film displays a reversible change in its color in response to a temperature change (Figure 6b). Furthermore, the color of this system may also be controllable by an electric field because of the sensitivity of the LC to electric fields.

CONCLUSIONS

In this study, I explained how to prepare a thermosensitive angle-independent colored system that operates on the basis of the Christiansen effect. Thus far, a few systems have been reported that enable the use of various dispersions of two different media for fabricating optical filters that operate via the Christiansen effect. In particular, our finding concerning a phase-separated porous polymer membrane filled with mixed

thermosensitive LCs exhibiting changes in color covering the whole visible region and an opaque milky color with temperature variation is a new colored material that is potentially useful for display systems (Figure 7). Because this system displays angle-independent color and can act as a multi-color PDLC, I believe that this system may be applicable for energy-saving multi-color displays.

Acknowledgements

This work was partially supported by a Grant-in-Aid for Scientific Research on Innovative Areas of “Fusion Materials: Creative Development of Materials and Exploration of Their Function through Molecular Control” (No. 2206) from the Ministry of Education, Culture, Sports, Science and Technology, Japan (MEXT).

References

1. Teshima M, Seki T, Kawano R, Takeuchi S, Yoshioka S, Takeoka Y. Preparation of structurally colored, monodisperse spherical assemblies composed of black and white colloidal particles using a micro-flow-focusing device. *Journal of Materials Chemistry C* **3**, 769-777 (2015).
2. Ohtsuka, Y., Seki, T. & Takeoka, Y. Thermally Tunable Hydrogels Displaying Angle-Independent Structural Colors. *Angewandte Chemie-International Edition* **54**, 15368-15373 (2015).
3. Yoshioka, S. & Takeoka, Y. Production of Colourful Pigments Consisting of Amorphous Arrays of Silica Particles. *Chemphyschem* **15**, 2209-2215 (2014).
4. Hirashima R, Seki T, Katagiri K, Akuzawa Y, Torimotoa T, Takeoka Y. Light-induced saturation change in the angle-independent structural coloration of colloidal amorphous arrays. *Journal of Materials Chemistry C* **2**, 344-348 (2014).
5. Takeoka Y, Yoshioka S, Teshima M, Takano A, Harun-Ur-Rashid M, Seki T. Structurally Coloured Secondary Particles Composed of Black and White Colloidal Particles. *Scientific Reports* **3** (2013).
6. Takeoka Y, Yoshioka S, Takano A, Arai S, Nueangnoraj K, Nishihara H Production of Colored Pigments with Amorphous Arrays of Black and White Colloidal Particles. *Angewandte Chemie-International Edition* **52**, 7261-7265 (2013).
7. Takeoka, Y. Stimuli-responsive opals: colloidal crystals and colloidal amorphous arrays for use in functional structurally colored materials. *Journal of Materials Chemistry C* **1**, 6059-6074 (2013).
8. Takeoka, Y. Angle-independent structural coloured amorphous arrays. *Journal of Materials Chemistry* **22**, 23299-23309 (2012).
9. Harun-Ur-Rashid M, Bin Imran A, Seki T, Ishi M, Nakamura H, Takeoka Y. Angle-Independent Structural Color in Colloidal Amorphous Arrays. *Chemphyschem* **11**, 579-583 (2010).
10. Takeoka, Y., Honda, M., Seki, T., Ishii, M. & Nakamura, H. Structural Colored Liquid Membrane without Angle Dependence. *Acs Applied Materials & Interfaces* **1**, 982-986 (2009).
11. Gotoh Y, Suzuki H, Kumano N, Seki T, Katagiri K, Takeoka Y. An amorphous

array of poly(N-isopropylacrylamide) brush-coated silica particles for thermally tunable angle-independent photonic band gap materials. *New Journal of Chemistry* **36**, 2171-2175 (2012).

12. Takeoka, Y. Fusion materials for biomimetic structurally colored materials. *Polymer Journal* **47**, 106-113 (2015).
13. Prum, R.O., Torres, R.H., Williamson, S. & Dyck, J. Coherent light scattering by blue feather barbs. *Nature* **396**, 28-29 (1998).
14. Dufresne ER, Noh H, Saranathan V, Mochrie SGJ, Cao H, Prum RO. Self-assembly of amorphous biophotonic nanostructures by phase separation. *Soft Matter* **5**, 1792-1795 (2009).
15. Noh H, Liew SF, Saranathan V, Mochrie SGJ, Prum RO, Dufresne ER, et al. How Noniridescent Colors Are Generated by Quasi-ordered Structures of Bird Feathers. *Advanced Materials* **22**, 2871-2880 (2010).
16. Shawkey, M.D. & Hill, G.E. Significance of a basal melanin layer to production of non-iridescent structural plumage color: evidence from an amelanotic Steller's jay (Cyanocitta stelleri). *Journal of Experimental Biology* **209**, 1245-1250 (2006).
17. Kumano, N., Seki, T., Ishii, M., Nakamura, H. & Takeoka, Y. Tunable Angle-Independent Structural Color from a Phase-Separated Porous Gel. *Angewandte Chemie-International Edition* **50**, 4012-4015 (2011).
18. Kumano N, Seki T, Ishii M, Nakamura H, Umemura T, Takeoka Y. Multicolor Polymer-Dispersed Liquid Crystals. *Advanced Materials* **23**, 884-888 (2011).
19. Christiansen, C. Untersuchungen über die optischen Eigenschaften von fein verteilten Körpern. *Ann. Phys. Chem.* **24**, 439-446 (1885).
20. Raman, C.V. The theory of the Christiansen experiment. *Proc. Ind. Acad. Sci.* **29**, 381-390 (1949).
21. Cauchy, M. *Philos. Mag. Ser.* **8**, 459-469 (1941).
22. Edo S, Okoshi K, Kang S, Tokita M, Kaneko T, Watanabe J. Unusual Swelling of HPC in Toluene Forming a Microspherical Domain Structure that Causes Christiansen Scattering Coloration. *Langmuir* **26**, 1743-1746 (2010).
23. Kato, T., Mizoshita, N., Kishomoto, K. *Angew. Chem. Int. Ed.* **45**, 38-68 (2006).
24. Kato, T., Hirai, Y., Nakaso, S. & Moriyama, M. Liquid-crystalline physical gels. *Chemical Society Reviews* **36**, 1857-1867 (2007).

25. Moriyama, M., Mizoshita, N. & Kato, T. Photopatterning of discotic liquid-crystalline gels. *Polymer Journal* **36**, 661-664 (2004).
26. Shishido, A. Rewritable holograms based on azobenzene-containing liquid-crystalline polymers. *Polymer Journal* **42**, 525-533 (2010).
27. Moriyama, M., Mizoshita, N., Yokota, T., Kishimoto, K. & Kato, T. Photoresponsive anisotropic soft solids: Liquid-crystalline physical gels based on a chiral photochromic gelator. *Advanced Materials* **15**, 1335-1338 (2003).
28. Ozaki, M., Shimoda, Y., Kasano, M. & Yoshino, K. Electric field tuning of the stop band in a liquid-crystal-infiltrated polymer inverse opal. *Advanced Materials* **14**, 514-518 (2002).
29. Kubo S, Gu ZZ, Takahashi K, Fujishima A, Segawa H, Sato O. Tunable photonic band gap crystals based on a liquid crystal-infiltrated inverse opal structure. *Journal of the American Chemical Society* **126**, 8314-8319 (2004).
30. Kubo S, Gu ZZ, Takahashi K, Ohko Y, Sato O, Fujishima A. Control of the optical band structure of liquid crystal infiltrated inverse opal by a photoinduced nematic-isotropic phase transition. *Journal of the American Chemical Society* **124**, 10950-10951 (2002).
31. Li, j., Wen, C. H., Gauza, S., Lu, R. B., Wu, S. T. Refractive Indices of Liquid Crystals for Display Applications. *J. Display Technol.* **1**, 51-61 (2005).

Figure Legends

Figure 1. a) SEM image of a porous polymer membrane composed of poly(MEO2). b) SEM image of a porous polymer membrane composed of the MMAA-BIS polymer. (Reproduced with permission from John Wiley and Sons.)

Figure 2. a) Solvent composition dependence of the transmission spectra and b) optical photographs of a porous polymer membrane composed of poly(MEO2) in different toluene-acetone mixed solvents at 20 °C. c) Transmission spectra of the porous polymer membrane in 85 wt% toluene were collected at various irradiation angles at 20 °C. (Reproduced with permission from John Wiley and Sons.)

Figure 3. a) Dispersion curves of pure toluene and the 10 wt% poly(MEO2) solution dissolved in toluene were compared at different temperatures. The intersection of these dispersion curves changed depending on the temperature. The transmission spectra of the porous polymer membrane composed of poly(MEO2) in toluene were obtained at different temperatures. b) λ_{max} values of the transmission spectra of the porous polymer membrane composed of poly(MEO2) in toluene at different temperatures were compared with the temperature-dependent intersections obtained by Cauchy's approximate equation. (Reproduced with permission from John Wiley and Sons.)

Figure 4. a) Dispersion curves of the MMAA-BIS polymer and of 5CB and 5PCH at several temperatures. The solid line was obtained by a least-squares fitting method. b) Conceptual scheme of the thermotropic LC. c) Temperature dependence of the refractive indices of 5CB and 5PCH measured at different wavelengths. In the right box, n_e and n_o are the refractive indices for the extraordinary ray and ordinary ray, respectively. The numeric data are quoted from Reference 31. (Reproduced with permission from John Wiley and Sons.)

Figure 5. DSC thermograms and optical photographs for LCs. (Reproduced with permission from John Wiley and Sons.)

Figure 6. Temperature dependence of the transmission spectra of the MMAA-BIS porous polymer membrane filled with LC mixtures and optical photographs. (Reproduced with permission from John Wiley and Sons.)

Figure 7. Conceptual scheme of the multi-color PDLC; n_e and n_o are refractive indices for the extraordinary ray and ordinary ray for the LC, respectively, and n_i and n_p are the refractive indices for the isotropic states of the LC and the polymer matrix, respectively. (Reproduced with permission from John Wiley and Sons.)

Angle-independent Colored Materials based on Christiansen effect using Phase Separated Polymer Membranes

Yukikazu Takeoka

Department of Molecular Design & Engineering, Nagoya University, Furo-cho, Chikusa-ku, Nagoya, 464-8603, Japan
E-mail: ytakeoka@apchem.nagoya-u.ac.jp

a)

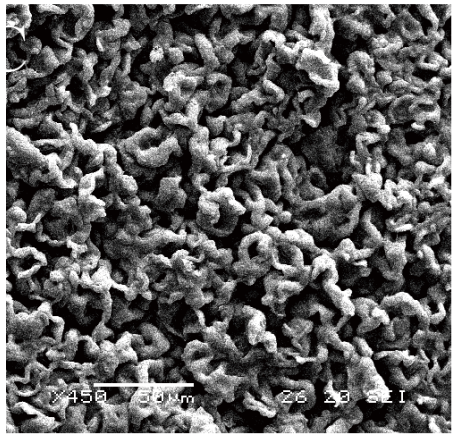

b)

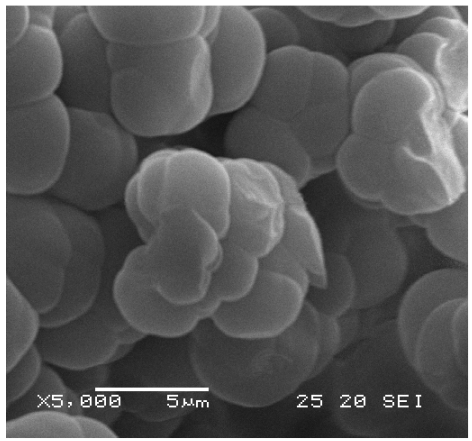

Figure 1

a)

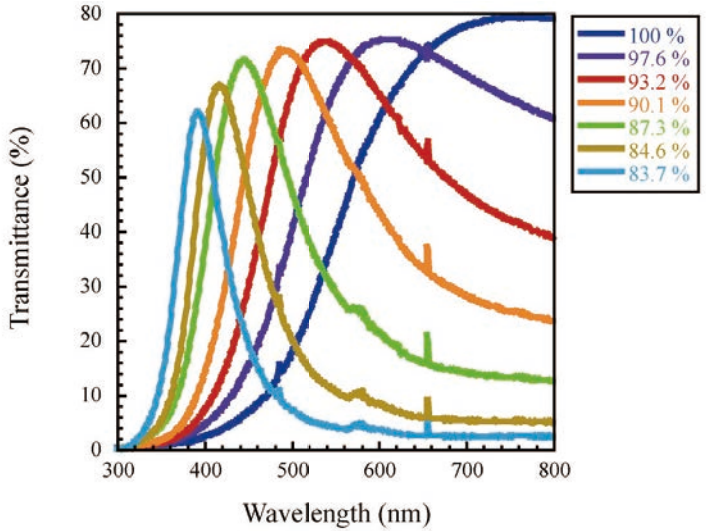
Transmittance (%)
Wavelength (nm)
100 %
97.6 %
93.2 %
90.1 %
87.3 %
84.6 %
83.7 %

b)

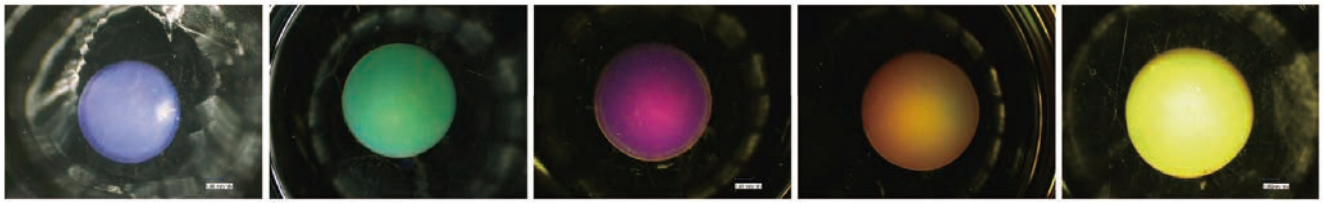
100 wt%
98.8 wt%
96.5 wt%
94.3 wt%
93.2 wt%

c)

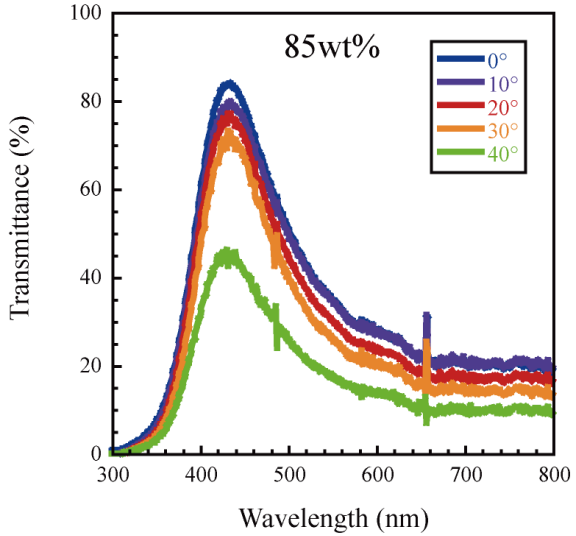
85wt%
0°
10°
20°
30°
40°
Transmittance (%)
Wavelength (nm)

Figure 2

a)

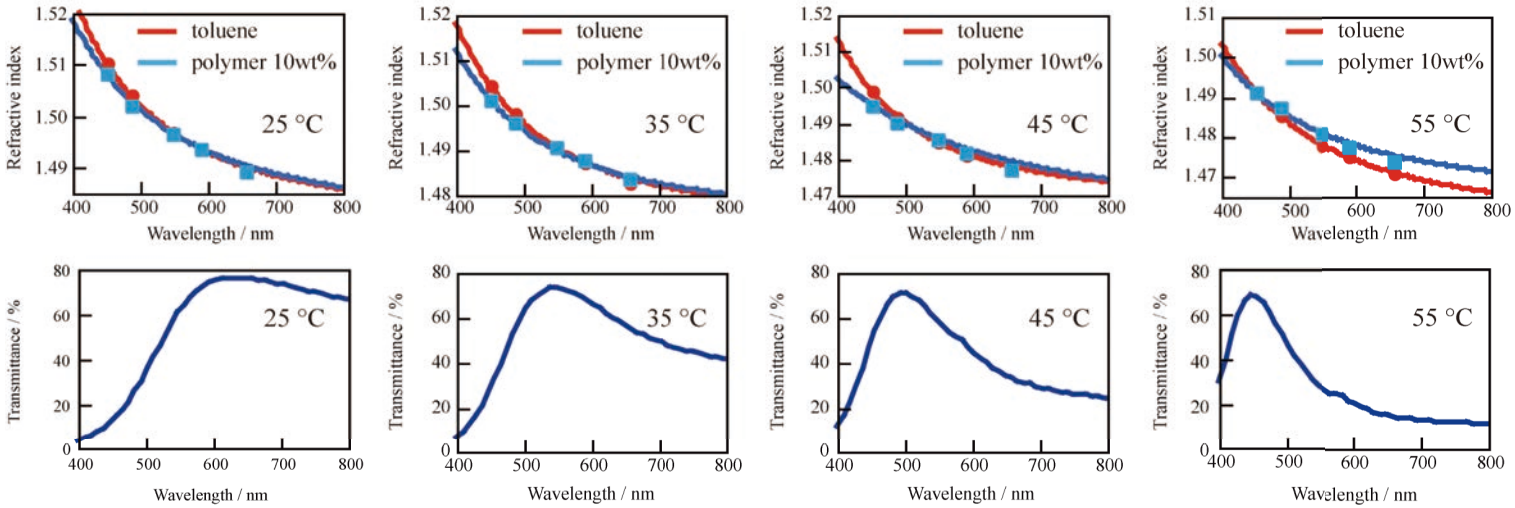
toluene
polymer 10wt%
25 °C
35 °C
45 °C
55 °C
Refractive index
Transmittance / %
Wavelength / nm

b)

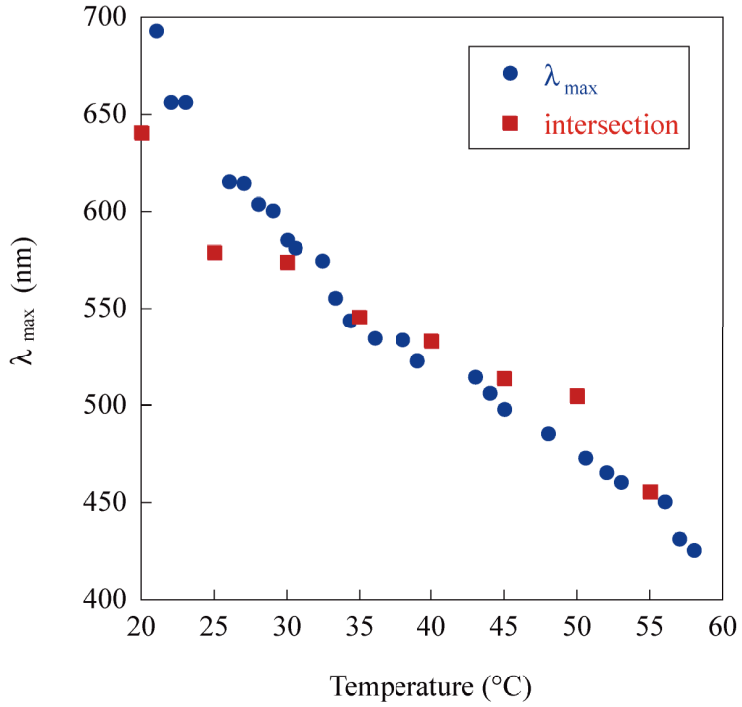
λ max
intersection
λ max (nm)
Temperature (°C)

Figure 3

a)

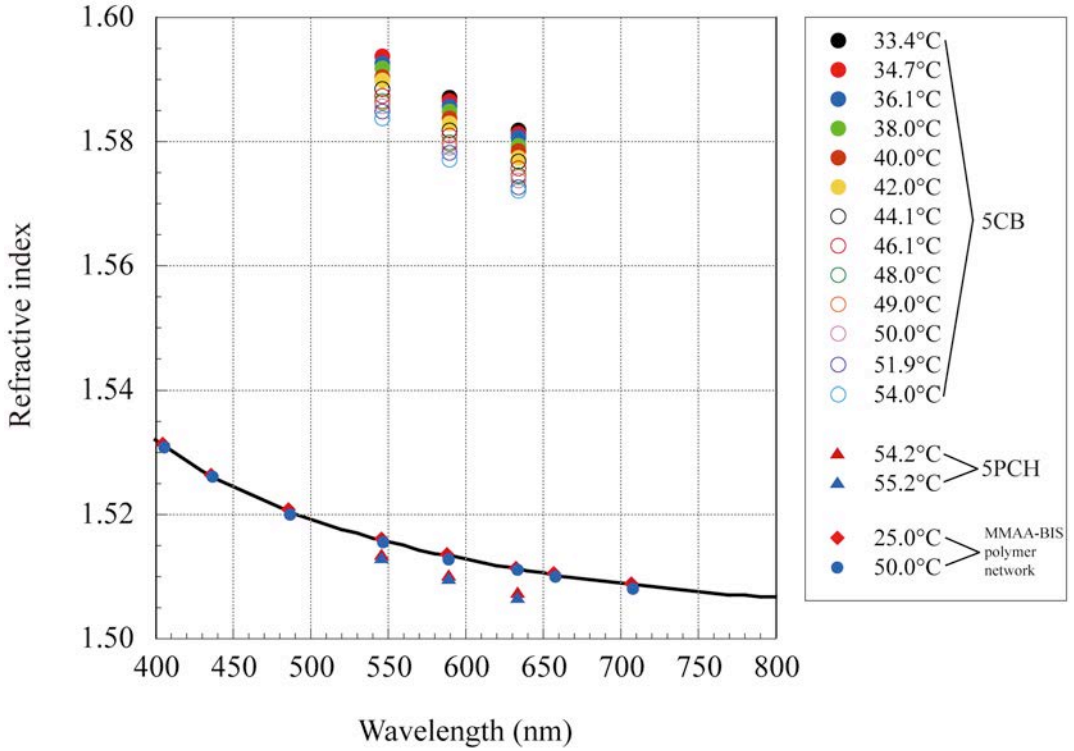
Refractive index
1.60
1.58
1.56
1.54
1.52
1.50
400
450
500
550
600
650
700
750
800
Wavelength (nm)
33.4°C
34.7°C
36.1°C
38.0°C
40.0°C
42.0°C
44.1°C
46.1°C
48.0°C
49.0°C
50.0°C
51.9°C
54.0°C
5CB
54.2°C
55.2°C
5PCH
25.0°C
50.0°C
MMAA-BIS polymer network

Figure 4a

b)

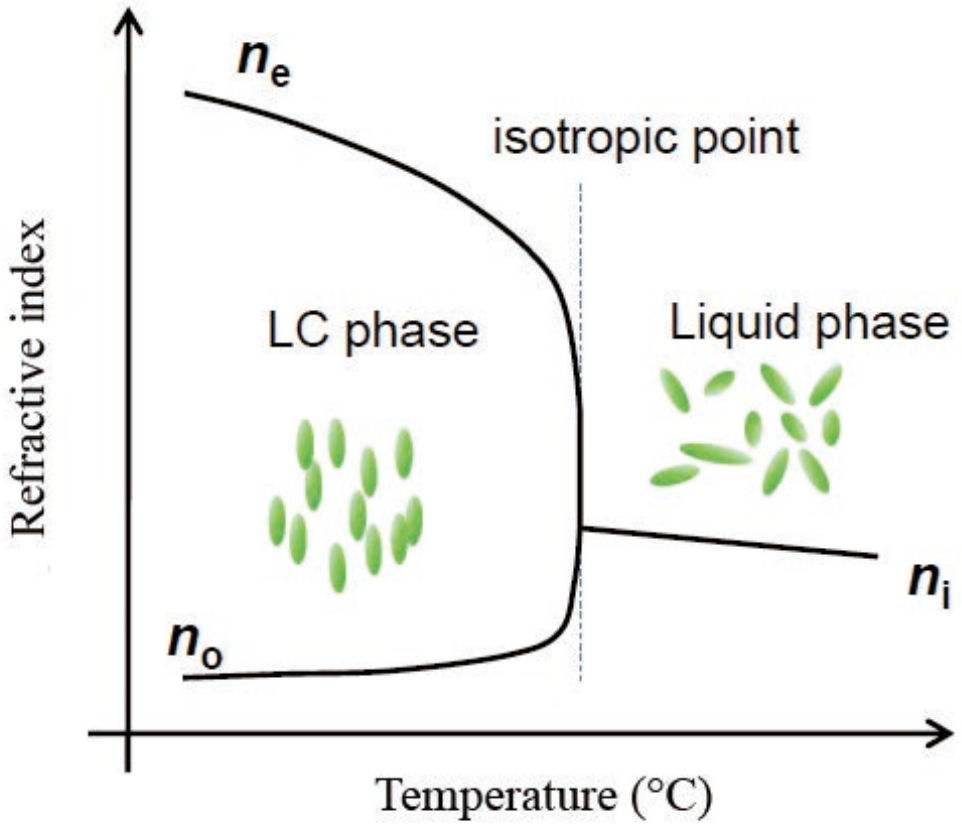
n_e
isotropic point
LC phase
Liquid phase
Refractive index
n_i
n_o
Temperature (°C)

Figure 4b

c)

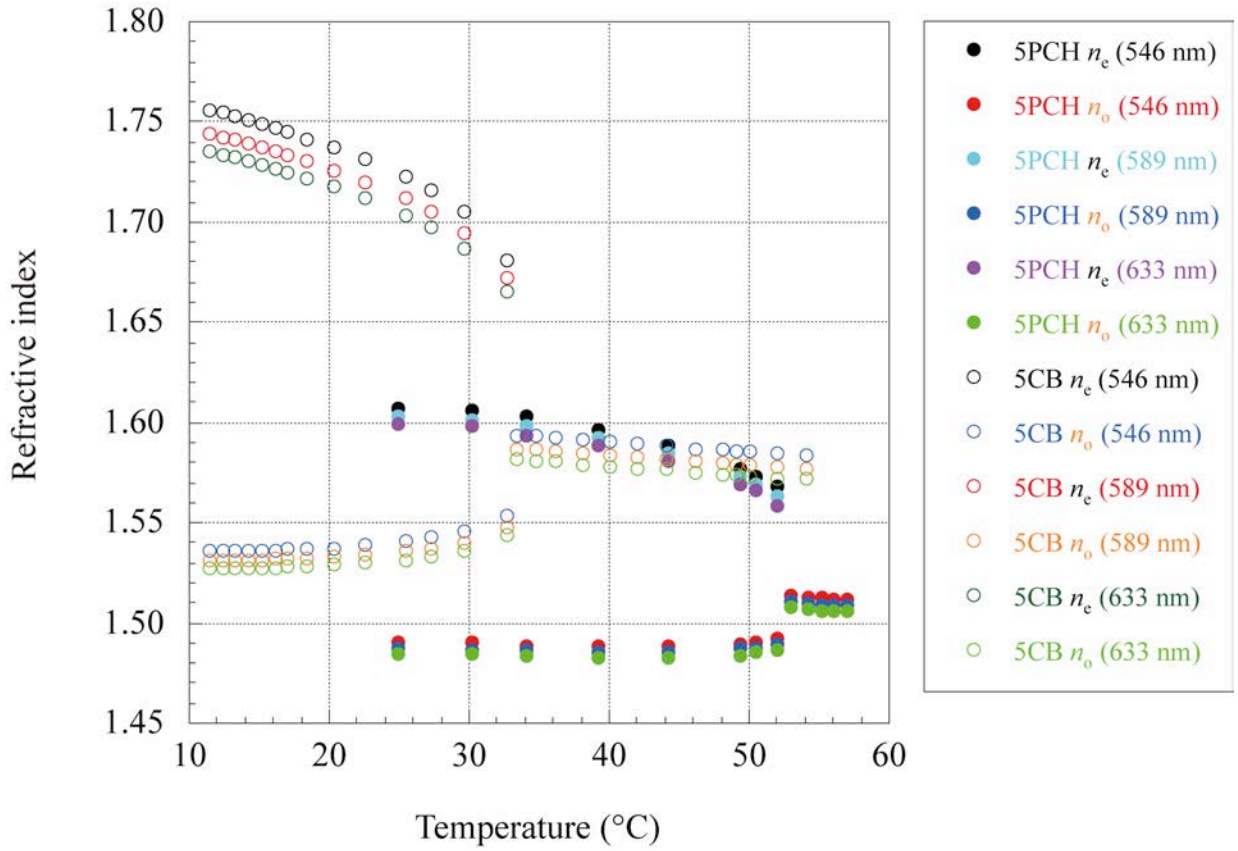
1.80
1.75
1.70
1.65
1.60
1.55
1.50
1.45
Refractive index
10
20
30
40
50
60
Temperature (°C)
5PCH n_e (546 nm)
5PCH n_o (546 nm)
5PCH n_e (589 nm)
5PCH n_o (589 nm)
5PCH n_e (633 nm)
5PCH n_o (633 nm)
5CB n_e (546 nm)
5CB n_o (546 nm)
5CB n_e (589 nm)
5CB n_o (589 nm)
5CB n_e (633 nm)
5CB n_o (633 nm)

Figure 4c

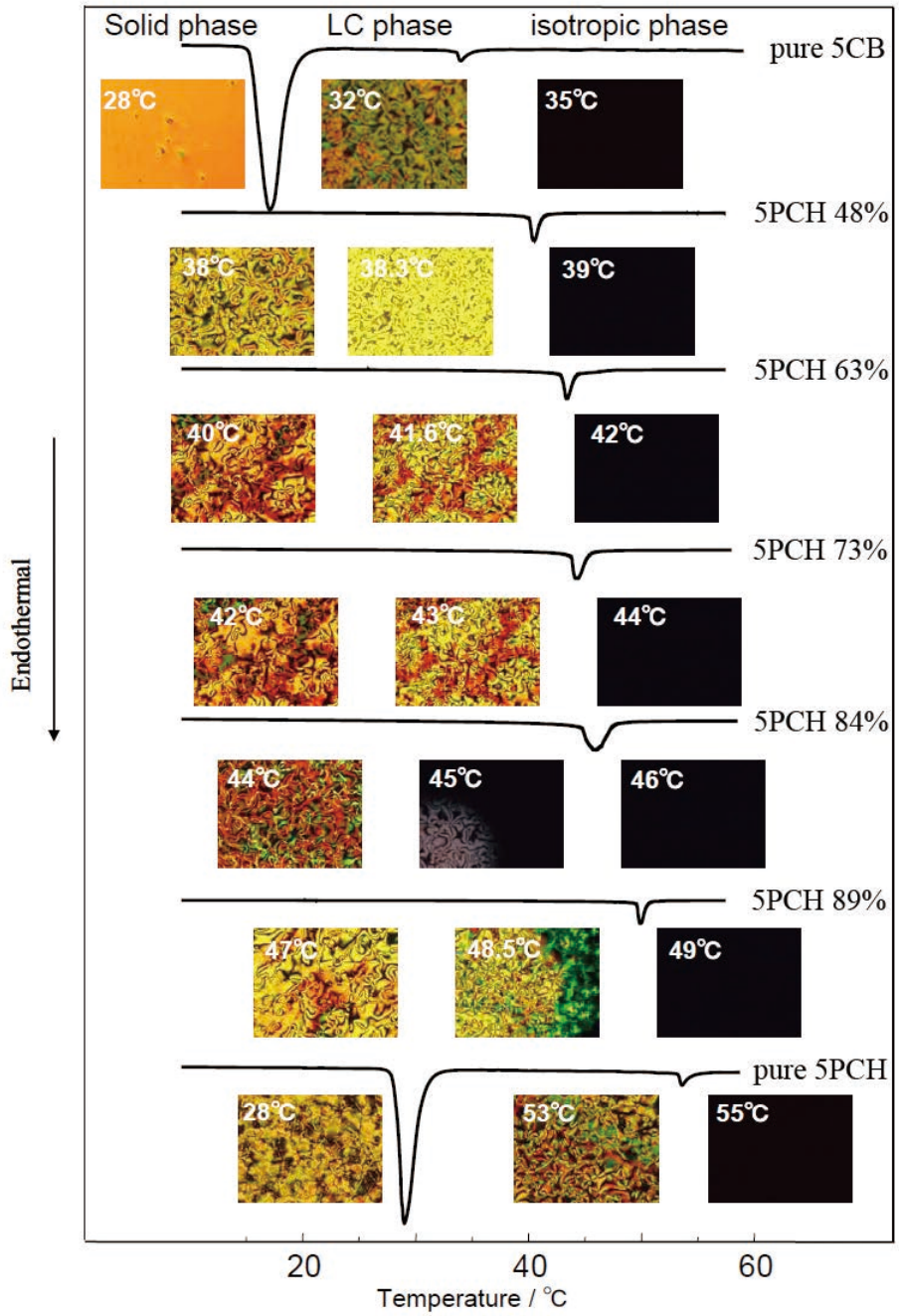
Solid phase
LC phase
isotropic phase
pure 5CB
28℃
32℃
35℃
5PCH 48%
38℃
38.3℃
39℃
5PCH 63%
40℃
41.6℃
42℃
5PCH 73%
42℃
43℃
44℃
5PCH 84%
44℃
45℃
46℃
5PCH 89%
47℃
48.5℃
49℃
pure 5PCH
28℃
53℃
55℃
Endothermal
20
40
60
Temperature / ℃

Figure 5

a)

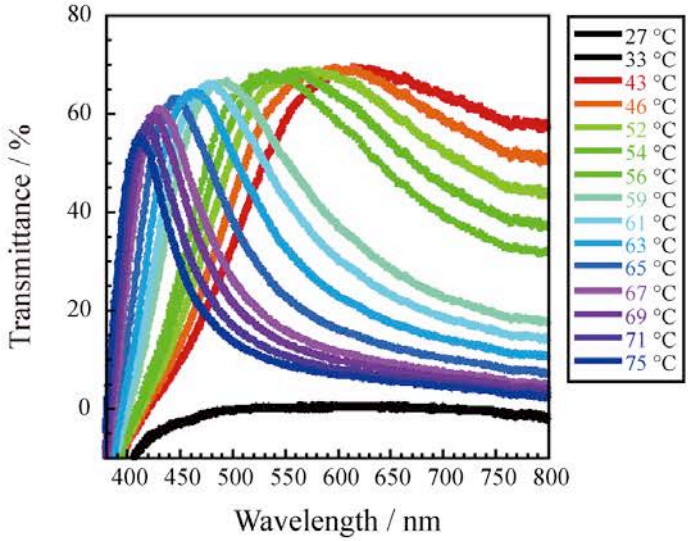
Transmittance / %
Wavelength / nm
0
20
40
60
80
400 450 500 550 600 650 700 750 800
27 °C
33 °C
43 °C
46 °C
52 °C
54 °C
56 °C
59 °C
61 °C
63 °C
65 °C
67 °C
69 °C
71 °C
75 °C

b)

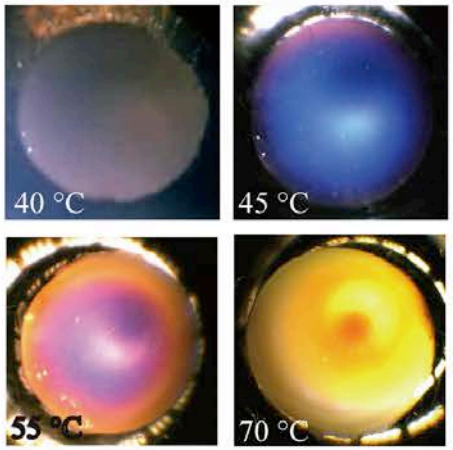
40 °C
45 °C
55 °C
70 °C

Figure 6

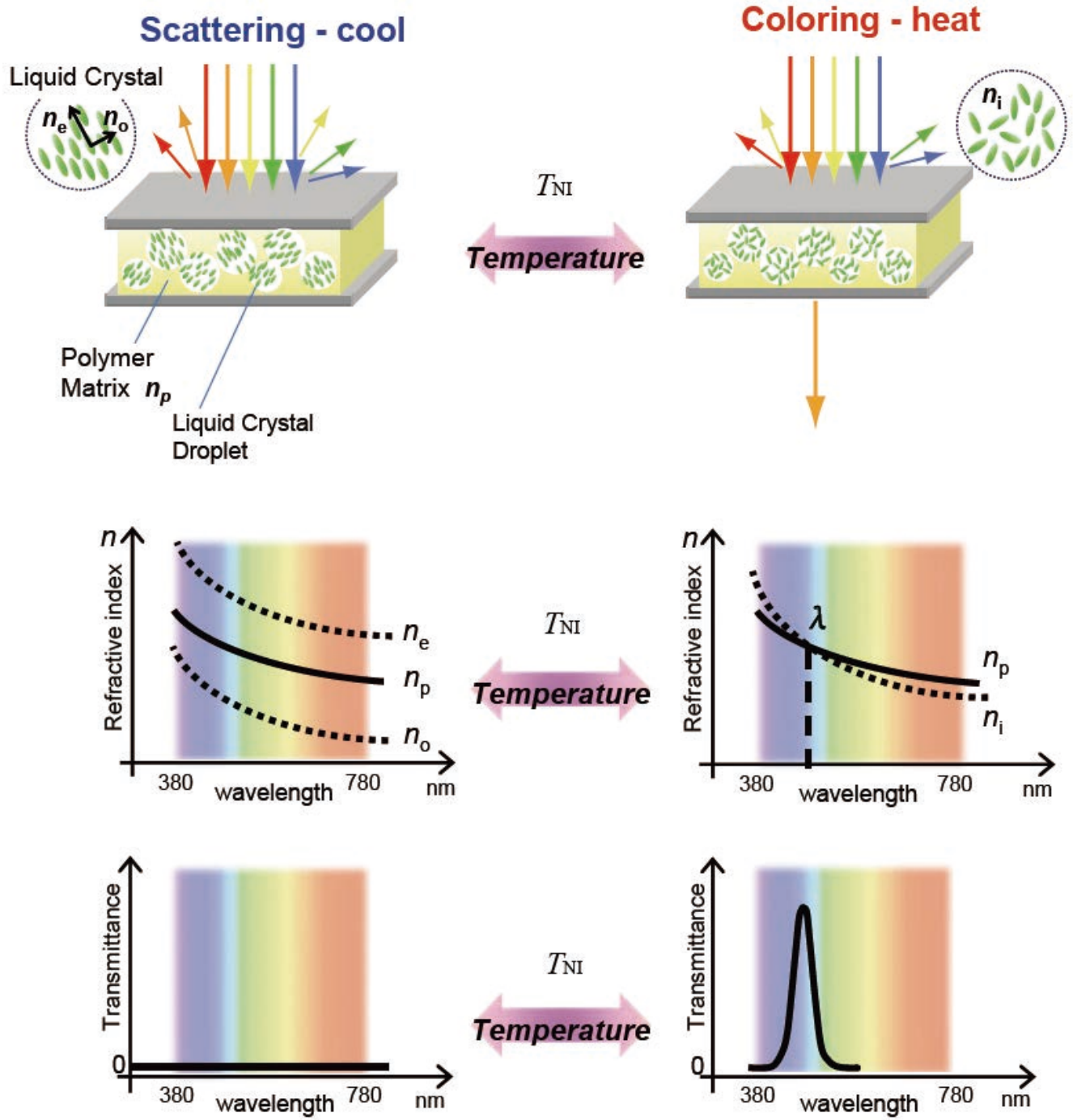
Scattering - cool
Coloring - heat
Liquid Crystal
n_e
n_o
n_i
T_{NI}
Temperature
Polymer Matrix n_p
Liquid Crystal Droplet
n
Refractive index
n_e
n_p
n_o
n_i
λ
380
wavelength
780
nm
Transmittance
0

Figure 7